Synthesis and Characterization of Palladium(II) Complexes with New Polydentate Nitrogen Ligands. Dynamic Behavior Involving Pd−N Bond Rupture. X-ray Molecular Structure of [{Pd(η^3-C_4H_7)}$_2$(Me-BPzTO)](4-$MeC_6H_4SO_3$) [Me-BPzTO = 4,6-Bis(4-methylpyrazol-1-yl)-1,3,5-triazin-2-olate]

Felipe Gómez-de la Torre, Antonio de la Hoz, Félix A. Jalón,* Blanca R. Manzano,*,† Antonio Otero, Ana M. Rodríguez, and M. Carmen Rodríguez-Pérez

Departamento de Química Inorgánica, Orgánica y Bioquímica, Facultad de Químicas, Campus Universitario, Universidad de Castilla-La Mancha, 13071 Ciudad Real, Spain

Aurea Echevarría and José Elguero

Instituto de Química Médica, CSIC, Juan de la Cierva, 3, 28006-Madrid, Spain

Received March 19, 1998

The ligands 2,4,6-tris(4-methylpyrazol-1-yl)-1,3,5-triazine (Me-TPzT), 2,4,6-tris(4-bromopyrazol-1-yl)-1,3,5-triazine (Br-TPzT), and 2-methoxy-4,6-bis(4-methylpyrazol-1-yl)-1,3,5-triazine (Me-BPzTOMe) have been synthesized and their reactions with some palladium derivatives explored. The palladium fragment [Pd(η^3-2-Me-C_3H_4)$(S)_2$]$^+$, S = acetone, reacts in acetone with Me-TPzT or Br-TPzT in a 3:1 molar ratio to generate new complexes in which two allylpalladium fragments are present and the TPzT ligands have been partially hydrolyzed: [{Pd(η^3-C_4H_7)}$_2$(X-BPzTO)]A, X-BPzTO = 4,6-bis[4-methyl(or bromo)pyrazol-1-yl]-1,3,5-triazin-2-olate (X = Me, A = BF_4, **1**; A = PF_6, **2**; A = CF_3SO_3, **3**; A = *p*-$MeC_6H_4SO_3$, **4**; X = Br, A = CF_3SO_3, **5**). When the ligand Me-BPzTOMe is made to react with only 1 equiv of the palladium solvate, compound **6**, [Pd(η^3-2-Me-C_3H_4)(Me-BPzTOMe)]CF_3SO_3, is isolated. Reaction of **6** with another 1 equiv of the palladium derivative leads to **3**. The intermediate **7**, [{Pd(η^3-2-Me-C_3H_4)}$_2$(Me-BPzTOMe)]CF_3SO_3, has been isolated as an almost pure compound. The reaction of Me-BPzTOMe with 1 equiv of [Pd(C_6F_5)$_2$(cod)] (cod = 1,5-cyclooctadiene) leads to the complex [Pd(C_6F_5)$_2$(Me-BPzTOMe)], **8**. Attention has been focused on the dynamic behavior, related with metallotropic phenomena, of the new complexes. ^{1}H NMR variable-temperature studies of complexes **1**, **6**, and **8** have been carried out. For **8**, only one static species is observed, while, for **1** and **6**, two isomers are detected at low temperature. Different $\Delta G_c^{\ddagger}$ activation energies at the coalescence temperature have been determined and are ascribed to processes implying Pd−N bond ruptures. For **6**, two different barriers are detected, corresponding to Pd−N(triazine) or Pd−N(pyrazole) bond ruptures. From the $\Delta G_c^{\ddagger}$ data, it is concluded that the main driving force of the hydrolysis process is the formation of a better coordinating ligand. The molecular structure of **4** has been determined by X-ray diffraction. The *meso* isomer, in which the two C−Me axes of the allylic groups are oriented in the same direction, is found in the solid state.

Introduction

In a coordination complex the electron-donor ability of the ligand is considered to be an essential aspect in its stabilization and reactivity modulation.[1] In this context, ligands such as phosphines, which allow a high versatility in donor ability and steric hindrance, have frequently been used in complex formation with transition metals of the last periodic series.[2] N-donor ligands that show less studied structural and reactivity patterns are receiving increased attention with these types of metals.[3] In particular, recent contributions[4] in the field of alkene polymerization and copolymerization using Pd and Ni complexes with N-donor ligands should be emphasized.

Polydentate nitrogen-donor ligands with sp^2-hybridized nitrogens are widely used, especially polypyrazolylborates[5] and polypyridines.[5b,6] Other aromatic polydentate N-donor ligands such as TPT[7] (2,4,6-tris-2-pyridyl-1,3,5-triazine) have also

† E-mail: bmanzano@qino-cr.uclm.es.

(1) *Comprehensive Coordination Chemistry*; Wilkinson, G., Gillard, R. D., McCleverty, J. A., Eds.; Pergamon: Oxford, U.K., 1987; Vol. 2.
(2) (a) McAuliffe, C. A.; Levason, W. *Phosphine, Arsine and Stibine Complexes of the Transition Elements*; Elsevier: Amsterdam, 1979. (b) Alyea, E. C. Catalytic Aspect of Metal Phosphine Complexes. *Adv. Chem. Ser.* **1982**, *No. 196*. (c) *Homogeneous Catalysis with Metal Phosphine Complexes*; Pignolet, L. H., Ed.; Plenum: New York, 1983.
(3) Togni, A.; Venanzi, L. M. *Angew. Chem., Int. Ed. Engl.* **1994**, *33*, 497 and references therein.
(4) (a) Brookhart, M.; Rix, F. C.; De Simone, J. M. *J. Am. Chem. Soc.* **1992**, *114*, 5894. (b) Brookhart, M.; Wagner, M. I. *J. Am. Chem. Soc.* **1994**, *116*, 3641. (c) Johnson, L. K.; Killian, C. M.; Brookhart, M. *J. Am. Chem. Soc.* **1995**, *117*, 6414. (d) Johnson, L. K.; Macking, S.; Brookhart, M. *J. Am. Chem. Soc.* **1996**, *118*, 267. (e) Rix, F. C.; Brookhart, M.; White, P. S. *J. Am. Chem. Soc.* **1996**, *118*, 4746. (f) Brookhart, M.; Wagner, M. I. *J. Am. Chem. Soc.* **1996**, *118*, 7219. (g) Killian, C. M.; Tempel, D. J.; Johnson, L. K.; Brookhart, M. *J. Am. Chem. Soc.* **1996**, *118*, 11664. (h) Milani, B.; Anzilutti, A.; Vicentini, L.; Sessanta, A. S.; Zangrando, E.; Geremia, S.; Mestroni, G. *Organometallics* **1997**, *16*, 5064.
(5) (a) Trofimenko, S. *Chem. Rev.* **1993**, *93*, 943. (b) Ward, M. D. *Annu. Rep. Prog. Chem. Inorg. Chem. Sect. A* **1994**, *91*, 317.

10.1021/ic980307n CCC: $15.00
Published on Web 12/01/1998

received considerable attention, especially in complex formation for charge-transfer studies and related properties. However, pyrazolyl-substituted triazines[8] have been explored to a lesser extent.

A relevant aspect in the reactivity of transition metal complexes is the effect that the metal may induce on organic molecules in such a way that a better ligand which is stabilized after its coordination is formed. The template-mediated macrocyclic synthesis[9] is a classical example but numerous cases related with this property of metals may be quoted.[1,10] Recently, several of us have reported[11] that the $[(\eta^3\text{-2-Me-}C_3H_4)Pd]^+$ cation is able to stabilize the $PO_2F_2^-$ anion, an intermediate in the hydrolysis of PF_6^-, by means of its coordination to the palladium center. In this paper we describe work that demonstrates that the $[Pd(\eta^3\text{-2-Me-}C_3H_4)(S)_2]^+$ solvate induces the hydrolysis of 1,3,5-triazine derivatives in such a way that these triazines are converted into ligands with better coordinating ability. The ligands used are pyrazole derivatives and contain several asymmetric chelating coordination sites. These ligands are 2,4,6-tris(4-methylpyrazol-1-yl)-1,3,5-triazine (Me-TPzT),[8b] 2,4,6-tris(4-bromopyrazol-1-yl)-1,3,5-triazine (Br-TPzT) (see Scheme 1), and 2-methoxy-4,6-bis(4-methylpyrazol-1-yl)-1,3,5-triazine (Me-BPzTOMe) (see Scheme 2). Considering the less basic character of the pyrazolyl fragments as compared with those of pyridine derivatives, the ligands used must lead, in principle, to a more facile fluxional behavior than that observed for TPT complexes. We have studied[12] the dynamic behavior of allylpalladium complexes, some of which contain chelate pyrazole-derived ligands, and we have shown the existence of Pd−N bond rupture, observable in the NMR time scale, that takes place preferentially at the less basic nitrogen atoms. In this paper, we report interesting examples in which, for a single compound, two simultaneous fluxional processes are detected with different energy barriers. We have also found that the difference lies in the Pd−N bond strength.

Scheme 1

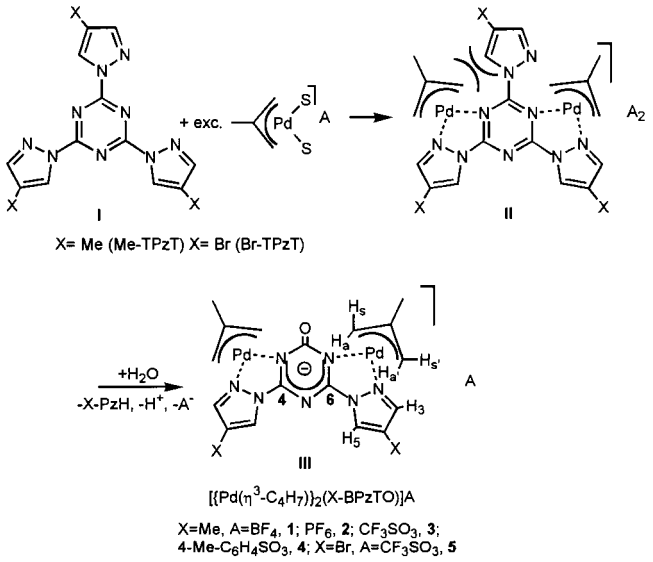

Experimental Section

General Comments. All manipulations were carried out under an atmosphere of dry oxygen-free nitrogen using standard Schlenk techniques. Solvents were distilled from the appropriate drying agents and degassed before use. $[(\eta^3\text{-2-Me-}C_3H_4)Pd(\mu\text{-Cl})]_2$[13] and $[Pd(C_6F_5)_2(cod)]$[14] were prepared as described in the literature. Elemental analyses were performed with a Perkin-Elmer 2400 microanalyzer. IR spectra were recorded as KBr pellets with a Perkin-Elmer PE 883 IR spectrometer. Mass spectra: VG Autospec instrument with FAB technique and nitrobenzyl alcohol as matrix. ^{1}H and ^{13}C NMR spectra were recorded on a Varian UNITY 300 spectrometer. Chemical shifts (ppm) are given relative to TMS. COSY spectra: standard pulse sequence with an acquisition time of 0.214 s, pulse width 10 μs, relaxation delay 1 s, number of scans 16, number of increments 512. The NOE difference spectra were recorded with the following acquisition parameters: spectral width 5000 Hz, acquisition time 3.27 s, pulse width 18 μs, relaxation delay 4 s, irradiation power 5−10 dB, number of scans 240. For variable temperature spectra, the probe temperature (±1 K) was controlled by a standard unit calibrated with a methanol reference. Free energies of activation were calculated[15] from the coalescence temperature (T_c) and the frequency difference between the

(6) (a) Juris, A.; Barigelletti, S.; Campagna, S.; Balzani, V.; Belser, P.; von Zelewsky, A. *Coord. Chem. Rev.* **1988**, 27. Some recent papers with terpyridine as a ligand in Pd or Pt complexes are: (b) Kvam, P. I.; Puzyk, M. V.; Cotlyr, V. S.; Balashev, K. P.; Songstad, J. *Acta Chem. Scand.* **1995**, *29*, 645. (c) Bailey, J. A.; Hill, M. G.; Marsh, R. E.; Miskowski, V. M.; Schaefer, W. P.; Gray, H. B. *Inorg. Chem.* **1995**, *34*, 4591. (d) Hill, M. G.; Bayley, J. A.; Miskowski, V. M.; Gray H. B. *Inorg. Chem.* **1996**, *35*, 4585. (e) Kvam, P. I.; Engebretsen, T.; Maartmannmoe, K.; Songstad, J. *Acta Chem. Scand.* **1996**, *50*, 107. (f) Kvam, P. I.; Puzyk, M. V.; Cotlyr, V. S.; Songstad, J.; Balashev, K. P. *Acta Chem. Scand.* **1996**, *50*, 6. (g) Abel, E. W.; Gelling, A.; Orrell, K. G.; Osborne, A. G.; Sik, V. *J. Chem. Soc., Chem. Commun.* **1996**, 2329. (h) Abel, E. W.; Orrell, K. G.; Osborne, A. G.; Pain, H. M.; Sik, V.; Husthouse, M. B.; Malik, K. M. A. *J. Chem. Soc., Chem. Commun.* **1996**, 253. (i) Abel, E. W.; Dimitrov, V. S.; Long, N. J.; Orrell, K. G.; Osborne, A. G.; Sik, V.; Hursthouse, M. B.; Mazid, A. A. *J. Chem. Soc., Chem. Commun.* **1993**, 291. (j) Schiavo, S. L.; Tresoldi, G.; Mezzasahna, A. M. *Inorg. Chim. Acta* **1997**, *36*, 251. (k) Yang, L.; Wimmer, F. L.; Wimmer, S., Zhao, J. X.; Braterman, P. S. *J. Organomet. Chem.* **1996**, *525*, 1.

(7) (a) Thomas, N. T.; Foley, B. L.; Rheingold, A. L. *Inorg. Chem.* **1988**, *27*, 3426. (b) Faus J.; Julve, M.; Amigó, J. M.; Debaerdemaeker, T. *J. Chem. Soc., Dalton Trans.* **1989**, 1681. (c) Folgado, J.-V.; Henke, W.; Allmann, R.; Stratemeier, H.; Beltrán-Porter, T.; Reinen, D. *Inorg. Chem.* **1990**, *29*, 2035. (d) Chirayil, S.; Hedge, V.; Jahng, Y.; Thummel, R. P. *Inorg. Chem.* **1991**, *30*, 2821. (e) Gupta, N.; Grover, N.; Neyhart, G. A.; Singh, P.; Thorp, H. *Inorg. Chem.* **1993**, *32*, 310. (f) Granifo, J. *Polyhedron* **1995**, *14*, 1593. (g) Berger, R. M.; Holcombe, J. R. *Inorg. Chim. Acta* **1995**, *232*, 217. (h) Berger, R. M.; Ellis, D. D., II. *Inorg. Chim. Acta* **1996**, *241*, 1. (i) Granifo, J. *Polyhedron* **1996**, *15*, 203. (j) Byers, P.; Chan, G. Y. S.; Drew, G. B.; Hudson, M. J.; Madic, C. *Polyhedron* **1996**, *15*, 2845. (k) Chan, G. Y. S.; Drew, G. B.; Hudson, M. J.; Isaacs, N. S.; Byers, P.; Madic, C. *Polyhedron* **1996**, *15*, 3385.

(8) (a) Reimlinger, H.; Noels, A.; Jadot, J.; van Overstraeten, A. *Chem. Ber.* **1979**, *103*, 1954. (b) Echevarría, A.; Elguero, J.; Llamas-Saiz, A. L.; Foces-Foces, C.; Schultz, G.; Hargittai, I. *Struct. Chem.* **1994**, *5*, 255. (c) Yang, C. Y.; Chen, X.-M.; Zhang, W.-H.; Chen, J.; Yang, Y.-S.; Gong, M.-L. *J. Chem. Soc., Dalton Trans.* **1996**, 1767. (d) Gelling, A.; Orrell, K. G.; Osborne, A. G.; Sik, V. *J. Chem. Soc., Dalton Trans.* **1996**, 3371.

(9) (a) Philp, D.; Stoddart, J. F. *Angew. Chem., Int. Ed. Engl.* **1996**, *35*, 1154. (b) Sessler, J. L.; Murai, T.; Lynch, V. *Inorg. Chem.* **1989**, *28*, 133. (c) Acholla, F. V.; Takusagawa, F.; Mertes, K. B. *J. Am. Chem. Soc.* **1985**, *107*, 6902. (d) Curtis, N. F. In *Comprehensive Coordination Chemistry*; Wilkinson, G., Gillard, R. D., McCleverty, J. A., Eds.; Pergamon: Oxford, U.K., 1982; Vol. 2, Chapter 21.1, p 899. (e) Ktakoviak, K.; Bradshaw, J. S.; Jiang, W.; Dalley, N. K.; Wu, G.; Izatt, R. M. *J. Org. Chem.* **1991**, *56*, 2675. (f) Melson, G. A.; Busch, D. H. *J. Am. Chem. Soc.* **1964**, *86*, 4834. (g) Blake, A. J.; Schröder, M. *Adv. Inorg. Chem.* **1990**, *35*, 1.

(10) *Reactions of Coordinated Ligands*; Braterman, P. S., Ed.; Plenum Press: New York, London, 1986.

(11) Fernández-Galán, R.; Manzano, B. R.; Otero, A.; Lanfranchi, M.; Pellinghelli, M. A. *Inorg. Chem.* **1994**, *33*, 2309.

(12) (a) Jalón, F. A.; Manzano, B. R.; Otero, A.; Rodríguez-Pérez, M. C. *J. Organomet. Chem.* **1995**, *494*, 179. (b) Elguero, J.; Fruchier, A.; de la Hoz, A.; Jalón, F. A.; Manzano, B. R.; Otero, A.; Gómez-de la Torre, F. *Chem. Ber.* **1996**, *129*, 589. (c) Fernández-Galán, R.; Jalón, F. A.; Manzano, B. R.; Rodríguez-de la Fuente, J.; Weissensteiner, W.; Kratky, C. *Organometallics* **1997**, *16*, 3758.

(13) (a) Dent, W. T.; Long, R.; Wilkinson, G. *J. Chem. Soc.* **1964**, 1585. (b) Tatsuno, Y.; Yoshida, T.; Seiotsuha. *Inorg. Synth.* **1979**, *19*, 220.

Scheme 2

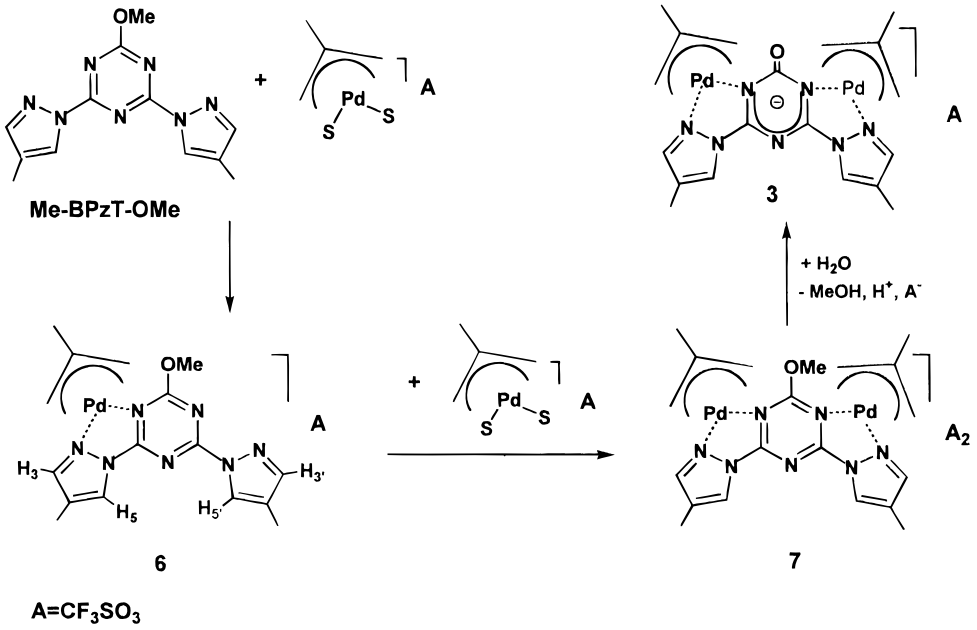

coalescing signals in the limit of slow exchange with the formula $\Delta G_c^{\ddagger} = aT(10.319 + \log T/\delta\nu)$. The estimated error in the calculated free energies of activation is 1.0−1.1 kJ mol^{-1}.

Preparation of Compounds. 2,4,6-Tris(4-methylpyrazol-1-yl)-1,3,5-triazine (Me-TPzT). An alternative method to that previously reported[8b] was used. A solution of 4-methylpyrazole (1.23 g, 15 mmol) in 20 mL of freshly distilled THF was added to a stirred suspension of sodium hydride (360 mg, 15 mmol) in THF. The mixture was stirred at room temperature for 21 h in order to complete deprotonation. 2,4,6-Trichloro-1,3,5-triazine (920 mg, 5 mmol) in 20 mL of THF was added to the above solution. A white precipitate formed immediately. After being stirred for 4 h, the solution was evaporated to dryness. The residue was extracted with distilled toluene (50 mL, 3 times). The solvent was removed under vacuum, and the resulting pale yellow solid washed with 25 mL of diethyl ether. Yield: 514 mg, 32%.

2,4,6-Tris(4-bromopyrazol-1-yl)-1,3,5-triazine·$^1/_2$CH$_2$Cl$_2$ (Br-TPzT). Br-TPzT was prepared from 4-bromopyrazole (500 mg, 3.4 mmol), sodium hydride (82 mg, 3.4 mmol), and 2,4,6-trichloro-1,3,5-triazine (209 mg, 1.13 mmol) by following the same procedure as described for Me-TPzT. Yield: 105 mg, 18%. Anal. Calcd for $C_{12}H_6Br_3N_9 \cdot {}^1/_2CH_2Cl_2$: C, 26.89; H, 1.26; N, 22.5. Found: C, 27.38; H, 0.95; N, 22.48.

2-Methoxy-4,6-bis(4-methylpyrazol-1-yl)-1,3,5-triazine (Me-BPzTOMe). Me-BPzTOMe was prepared from 4-methylpyrazole (1.0 g, 12 mmol), sodium hydride (290 mg, 12 mmol), and 2,4-dichloro-6-methoxy-1,3,5-triazine (1.11 g, 6 mmol) by following the same procedure as described for Me-TPzT. Yield: 600 mg, 37%. Anal. Calcd for $C_{12}H_{13}N_7O$: C, 53.13; H, 4.83; N, 36.14. Found: C, 52.97; H, 4.91; N, 36.22.

[{(η^3-2-Me-C$_3$H$_4$)Pd}$_2$(Me-BPzTO)]BF$_4$ (1). [(η^3-2-Me-C$_3$H$_4$)Pd(μ-Cl)]$_2$ (120 mg, 0.3 mmol) was dissolved in 15 mL of distilled acetone. AgBF$_4$ (120 mg, 0.6 mmol) was then added to the above solution. After being stirred for 6 h at room temperature in the dark, the solution was filtered through a plug of Celite and cooled with an ice bath, and then Me-TPzT (65 mg, 0.2 mmol) was added. The product appeared as a precipitate, and the mixture was left stirring for 5 h. The solid was filtered off and the residue washed with 10 mL of diethyl ether. Yield: 91 mg, 68%. Anal. Calcd for $C_{19}H_{24}BF_4N_7OPd_2$: C, 34.26; H, 3.63; N, 14.72. Found: C, 34.20; H, 3.61; N, 14.27.

[{(η^3-2-Me-C$_3$H$_4$)Pd}$_2$(Me-BPzTO)]PF$_6$·(CH$_3$)$_2$CO (2), [{(η^3-2-Me-C$_3$H$_4$)Pd}$_2$(Me-BPzTO)]CF$_3$SO$_3$·$^1/_2$(CH$_3$)$_2$CO (3), [{(η^3-2-Me-C$_3$H$_4$)Pd}$_2$(Me-BPzTO)](*p*-MeC$_6$H$_4$SO$_3$) (4), and [{(η^3-2-Me-C$_3$H$_4$)-Pd}$_2$(Br-BPzTO)]CF$_3$SO$_3$ (5). These compounds were prepared in a similar way to **1** from [(η^3-2-Me-C$_3$H$_4$)Pd(μ-Cl)]$_2$, the corresponding silver salt, and Me-TPzT (**2**−**4**) or Br-TPzT (**5**). **2**: Yield 84%. Anal. Calcd for $C_{19}H_{24}F_6N_7OPPd_2 \cdot C_3H_6O$: C, 33.78; H, 3.87; N, 12.53. Found: C, 33.77; H, 3.83; N, 12.14. **3**: Yield 88%. Anal. Calcd for $C_{20}H_{24}F_3N_7O_4Pd_2S \cdot {}^1/_2C_3H_6O$: C, 34.10; H, 3.59; N, 12.95. Found: C, 33.85; H, 3.62; N, 13.00. **4**: Yield 92%. Anal. Calcd for $C_{26}H_{31}N_7O_4Pd_2S$: C, 41.62; H, 4.16; N, 13.06. Found: C, 41.42; H, 3.89; N, 12.76. **5**: Yield: 68%. Anal. Calcd for $C_{18}H_{18}Br_2F_3N_7O_4Pd_2S$: C, 27.50; H, 2.64; N, 10.70; S, 3.50. Found: C, 27.10; H, 2.27; N, 10.88; S, 3.61.

[(η^3-2-Me-C$_3$H$_4$Pd)(Me-BPzTOMe)]CF$_3$SO$_3$ (6). [(η^3-2-Me-C$_3$H$_4$)-Pd(μ-Cl)]$_2$ (143 mg, 0.36 mmol) was dissolved in 15 mL of distilled acetone. To the above solution was added AgCF$_3$SO$_3$ (186 mg, 0.73 mmol). After being stirred for 6 h at room temperature in the dark, the solution was filtered through a plug of Celite, and Me-BPzTOMe (197 mg, 0.73 mmol) was added. The mixture was left stirring for 12 h; then the solvent was removed under vacuum and the residue washed with 10 mL of diethyl ether. Yield: 323 mg, 77%. Anal. Calcd for $C_{17}H_{20}F_3N_7O_4PdS$: C, 35.09; H, 3.46; N, 16.85. Found: C, 35.42; H, 4.01; N, 16.85.

[{(η^3-2-Me-C$_3$H$_4$)Pd}$_2$(Me-BPzTOMe)](CF$_3$SO$_3$)$_2$ (7). An enriched sample of this compound was obtained by the following procedure. [(η^3-2-Me-C$_3$H$_4$)Pd(μ-Cl)]$_2$ (20.3 mg, 0.051 mmol) was dissolved in 15 mL of distilled acetone. To the above solution was added AgCF$_3$-SO$_3$ (26.4 mg, 0.102 mmol). After being stirred for 12 h at room temperature in the dark, the solution was filtered through a plug of Celite and cooled to −78 °C with a dry ice/acetone bath, and then **6** (50 mg, 0.086 mmol) was added. After the solution was stirred for 1 min, the solvent was removed under vacuum and the product washed with 5 mL of cooled diethyl ether. Satisfactory analysis could not be obtained.

[(Pd(C$_6$F$_5$)$_2$)(Me-BPzTOMe)] (8). [Pd(C$_6$F$_5$)$_2$(cod)] (92.5 mg, 0.17 mmol, cod = 1,5-cyclooctadiene) was dissolved in 20 mL of distilled THF. To the above solution was added Me-BPzTOMe (45.7 mg, 0.17 mmol). After the solution was stirred for 45 min at room temperature, the solvent was removed and the residue washed with 10 mL of hexane. Yield: 97.8 mg, 82%. Anal. Calcd for $C_{24}H_{13}F_{10}N_7OPd$: C, 40.50; H, 1.84; N, 13.77. Found: C, 40.61; H, 1.50; N, 14.11. ^{19}F NMR at 295 K in acetone-d_6: F_{ortho}, −118.04 (m), −117.67 (m); F_{para}, −160.92 (t), −162.54 (t), J_{FF} = 21.4 Hz; F_{meta}, −164.05 (m), −165.84 (m).

(14) Espinet, P.; Martínez-de Ilarduya, J. M.; Pérez-Briso, C.; Casado, A. L.; Alonso, M. A. *J. Organomet. Chem.* **1998**, *551*, 9.
(15) Sandström, J. *Dynamic NMR Spectroscopy*; Academic Press: London, 1982.

Table 1. ^{1}H NMR Data for Me-TPzT, Br-TPzT, and Me-BpzTOMe Ligands and **1**−**8** Complexes[a] (δ, ppm; Solvent, Acetone-d_6)

compd	temp (K)	H_3	H_5	X	O*Me*	H_s	$H_{s'}$	H_a	$H_{a'}$	CH_3
Me-TPzT	295	7.81	8.64	2.18						
Br-TPzT	295	7.88	8.77							
Me-BPzTOMe	295	7.74	8.52	2.18	4.18					
1−**4**	295	8.24	8.78	2.19		4.63 (bs)	4.41 (bs)	3.31 (bs)		2.26
1−**4** M	218	8.25	8.76	2.11		4.51	4.43	3.36	3.30	2.15
1−**4** m	218	8.29	8.79	2.15		4.55	4.43	3.34	3.28	2.18
5	295	8.56	9.35			4.61		3.39		2.21
6	295	7.93[c] (bs)	8.74[c] (bs)	2.19	4.40	4.60		3.44		2.23
		8.37 (bs)	8.87 (bs)	2.26						
6M[b]	183	7.98[c]	8.88[c]	2.11	4.30	4.63		3.45		2.17
		8.43	9.16	2.20						
6m[b]	183	8.02[c]	8.73[c]	2.12	4.33	4.64		3.45		2.17
		8.45	8.79	2.26						
7	295	8.37	9.07	2.24	4.56	4.42 (bs)		3.39 (bs)		2.27
8	295	7.23[c]	8.30[c]	2.18	3.87					
		7.83	8.46	2.21						

[a] See Scheme 1 for numbering scheme. [b] M = major isomer; m = minor isomer. [c] Signals corresponding to free pyrazol groups ($H_{3'}$ or $H_{5'}$).

Table 2. ^{13}C NMR Data for Me-TPzT, Br-TPzT, and Me-BPzTOMe Ligands and **1**−**8** Complexes[a] (*T*, 295 K; δ, ppm; Solvent, Acetone-d_6 If Not Indicated)

									allylic signals		
compd	C_2	C_4	C_6	$C_{3'}$	$C_{4'}$	$C_{5'}$	X	O*Me*	−C=	CH_2	CH_3
Me-TPzT		162.9		128.8	120.6	146.5	7.8				
Br-TPzT[b]	*c*	*c*	*c*	131.3	98.7	146.0					
Me-BPzTOMe	*c*	*c*	*c*	129.2	121.5	147.5	9.3	56.6			
Me-BPzTOMe[d]	172.7	162.3		126.9	120.4	146.8	8.7	55.7			
1−**4**	156.0	161.4		129.5	122.2	148.6	7.7		131.4	59.7 (bs), 61.5 (bs)	22.2
5	*c*	*c*	*c*	133.2	100.4	149.1			122.3	62.7 (bs)	23.3
6	*c*	*c*	*c*	130.4	123.5	149.7	8.8	58.5	*c*	62.7 (bs)	23.1
				130.8	124.1	150.9					
8	171.3	163.3	163.0	129.7	123.1	148.1	8.9	57.5		C_6F_5 ring	
				130.7	123.9	149.4				120−150 (bs)	

[a] See Scheme 1 for numbering scheme. [b] In dmso-d_6. [c] Not observed. [d] In chloroform-*d*.

Table 3. Observed Coalescences and Calculated Free Activation Energies after the Variable-Temperature ^{1}H NMR Spectra of **1** (Left) and **6** (Right)[a]

coalescence[b]	T_c (K)[c]	$\Delta G_c^{\ddagger}$ (kJ/mol)[d]	coalescence[b]	T_c (K)[c]	$\Delta G_c^{\ddagger}$ (kJ/mol)[d]
H_3(pz)	243	53.6	H_3 (pz)	208	46.0
H_5(pz)	253	54.4	$H_{3'}$ (pz)	213	46.1
1 + 2 H_{syn}	253	54.6	MeO	218	46.4
3 + 4 H_{syn}	263	58.0	$H_{5'}$ (pz)	228	46.6
(1 + 2) + (3 + 4) H_{syn}	302	60.9	H_5 (pz)	238	46.9
1 + 2 H_{anti}	258	56.0	$H_5 + H_{5'}$	303	62.8
(1 + 2) + (3 + 4) H_{anti}	288	60.5	$H_3 + H_{3'}$	328	65.1

[a] Acetone-d_6 solution. For the allylic protons 1−4 refer to the signals in the order of increasing frequency. [b] See Schemes 1 and 2 for labeling scheme. [c] Coalescence temperatures. [d] Free activation energies at the coalescence temperatures calculated by $\Delta G_c^{\ddagger} = aT[9.972 + \log(T/\delta\nu)]$ ($a = 1.914 \times 10^{-2}$).

Table 4. Crystal Data for Compound **4**

chem formula	$C_{26}H_{31}N_7O_4Pd_2S\cdot CH_2Cl_2$
fw	835.36
T	25(2) °C
λ	0.710 70 Å
space group	*A*2/*m*
a	9.7640(10) Å
b	16.1890(10) Å
c	21.175(5) Å
β	99.040(10)°
V	3305.5(9) Å^3
Z	8
ρ_{calcd}	1.679 g/cm^3
μ	13.56 cm^{-1}
*R*1[a]	0.0523
w*R*2[a]	0.1328

[a] $R1 = \sum||F_o| - |F_c||/\sum|F_o|$; $wR2 = [\sum[w(F_o^2 - F_c^2)^2]/\sum[w(F_o^2)^2]]^{0.5}$.

X-ray Structure Determination of 4. Crystals of compound **4** suitable for X-ray diffraction were obtained by crystallization from methylene chloride/hexane and are air stable. Crystallographic data are given in Table 4. Reflections were collected at 25 °C on a Nonius MACH3 diffractometer equipped with graphite-monochromated radiation ($\lambda = 0.7107$ Å). Unit cell dimensions were obtained by least-squares fit of the 2θ values of 25 high-order reflections by using the MACH3 centering routines. The intensities of 4121 reflections were collected ($2 < \theta < 28$); of these only 2330 reflections obeyed the condition $I > 2\ \sigma(I)$. Data were corrected in the usual fashion for Lorentz and polarization effects, and an empirical absorption correction (Ψ scan) was applied (range of transmission factor 0.459−1.000). The space group was determined from the systematic absences (hkl, $k + l = 2n + 1$; $0kl$, $k + l = 2n + 1$; $h0l$, $l = 2n + 1$; $hk0$, $k = 2n + 1$; $0k0$, $k = 2n + 1$; $00l$, $l = 2n + 1$). The structure was solved by direct methods (SIR 92)[16] and refinement on F^2 was carried out by full-matrix least-squares analysis (SHELXL-93).[17] A number of cycles of refinement with isotropic thermal parameters, followed by difference synthesis, enabled location of all the non-hydrogen atoms along with three unexpected peaks, which were attributed to CH_2Cl_2 from the recrystallization mixture. The occupation factors for these sites were fixed at 0.5 in the subsequent refinement procedure. The CH_2Cl_2 half molecule was found to be disordered across the mirror plane, and as a result, its geometry is imprecise. For the final cycles of refinement all non-hydrogen atoms were refined anisotropically, while hydrogen atoms were included in calculated positions but not refined. No extinction

(16) Altomare, A.; Cascarano, G.; Giacovazzo, C.; Guagliardi, A.; Burla, M. C.; Polidori, G.; Camalli, M. *J. Appl. Crystallography* **1994**, 435.
(17) Sheldrick, G. M. *Program for the Refinement of Crystal Structures from Diffraction Data*; University of Göttingen: Göttingen, Germany, 1993.

correction was found to be necessary. The scattering factors used, corrected for the real and imaginary parts of the anomalous dispersion, were taken from the literature.[18] Upon convergence the final Fourier difference map showed no significant peaks. Final disagreement indices are $R = 0.052$, $R_w = 0.1328$, GOF = 1.061, and largest difference peak and hole 0.756 and -0.704 e·Å^{-3}.

Results and Discussion

Synthesis of the New Ligands and Complexes. Me-TPzT,[8b] Br-TPzT, and Me-BPzTOMe were prepared from the corresponding pyrazolate anion and 2,4,6-trichloro-1,3,5-triazine (in the cases of Me-TPzT and Br-TPzT) or 2,4-dichloro-6-methoxy-1,3,5-triazine (Me-BPzTOMe).

Reaction of $[Pd(\eta^3\text{-}2\text{-}Me\text{-}C_3H_4)(S)_2]^+$ (S = acetone), prepared by reaction of $[Pd(\eta^3\text{-}2\text{-}Me\text{-}C_3H_4)(\mu\text{-}Cl)]_2$[13] with the appropriate silver salt, with Me-TPzT or Br-TPzT in acetone in a 3:1 molar ratio generated the complexes $[\{Pd(\eta^3\text{-}C_4H_7)\}_2(X\text{-}BPzTO)]A$ (X-BPzTO = 4,6-bis(4-methylpyrazol-1-yl)-1,3,5-triazin-2-olate (Me-BPzTO), A = BF_4 (**1**), PF_6 (**2**), CF_3SO_3 (**3**), 4-Me-C_6H_4-SO_3 (**4**); X-BPzTO = 4,6-bis(4-bromopyrazol-1-yl)-1,3,5-triazin-2-olate (Br-BPzTO), A = CF_3SO_3 (**5**)) (Scheme 1) in high yields (80%). These complexes were slightly soluble in acetone, and they were air stable in the solid state. However, on standing of solutions for prolonged periods, an evolution to give free 4-Me- or 4-Br-pyrazole was observed. When the corresponding reaction was carried out in a 1:1 or 2:1 molar ratio, the same complexes were always obtained, although in lower yields and with free ligand remaining in solution.

Surprisingly, two allylpalladium fragments were incorporated and the TPzT ligands were partially hydrolyzed, with the corresponding pyrazole being detected by ^{1}H NMR in solution.

Although *N*-pyrazole fragments are good leaving groups, the X-TPzT ligands were stable in solution. Consequently, the allylpalladium fragment must induce, in some way, the hydrolysis process by adventitious water[19] present in the reaction mixture. In 1,3,5-triazine derivatives it is known that such a hydrolysis takes place by nucleophilic displacement in a stepwise process[20] or by a single transition state consistent with simultaneous bond formation and fission (A_ND_N).[21] An intermediate suggesting this type of nucleophilic attack has been isolated in pyridine-substituted triazines.[21d] The ease of substitution of pyrazole in these complexes may be explained (i) as a consequence of the steric hindrance of the allyl group when two palladium fragments are coordinated (see Scheme 1, intermediate II) or (ii) by a special stability of the hydrolyzed ligand coordinated to two allylpalladium groups. To obtain complementary information about the driving force for this hydrolysis we performed the reaction with a new ligand, 2-methoxy-4,6-bis(4-methylpyrazol-1-yl)-1,3,5-triazine (Me-BPzTOMe), in which a pyrazolyl group has been replaced by a methoxy group. The methoxy group is less sterically demanding than the pyrazole ring and also a poorer leaving group. However, on using a Pd:ligand ratio of 2:1 (A = CF_3SO_3), the same complex (**3**) was obtained and only the loss of the methoxy group was observed. If one takes into account the smaller steric hindrance induced by the methoxy group in a dinuclear intermediate (type II, Scheme 1), the special stability of the X-BPzTO cationic compound must play a predominant role in the evolution of these reactions.

Scheme 3

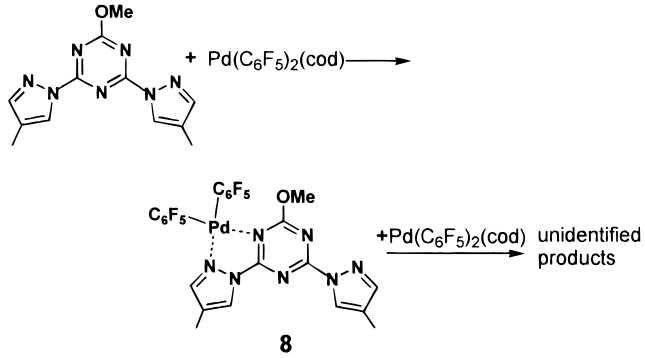

The intermediate **7**, $[\{Pd(\eta^3\text{-}C_4H_7)\}_2(Me\text{-}BPzTOMe)](CF_3SO_3)_2$, was detected by monitoring the reaction by ^{1}H NMR spectroscopy at low temperature as the major component in a mixture with **3**. It was observed that **7** evolves to **3** and methanol. Complex **7** was isolated as an almost pure compound after only a short reaction time at low temperature, but in solution **7** evolves quickly to **3**.

In contrast to the behavior observed with Me-TPzT, when Me-BPzTOMe is reacted with 1 equiv of the palladium solvate, complex $[Pd(\eta^3\text{-}C_4H_7)(Me\text{-}BPzTOMe)]CF_3SO_3$ (**6**) with one palladium center and a nonhydrolyzed ligand was isolated (see Scheme 2). Reaction of **6** with a second 1 equiv of the palladium derivative leads to **3**. In agreement with all these observations, complexes **6** and **7** are reasonable intermediates in the formation of **3** when ligand Me-BPzTOMe is used, as shown in Scheme 2, the dicationic complex **7** being more prone to nucleophilic attack than the monocationic complex **6**. A similar pathway may be assumed for reactions with X-TPzT ligands. The difference in behavior between BPzTOMe and X-TPzT complexes must be due to the better leaving character of Pz^- in comparison with MeO^-.

To show the influence of the Pd fragment on the hydrolysis process, the reactions of Me-BPzTOMe with 1 and 2 equiv of $[Pd(C_6F_5)_2(cod)]$ (cod = 1,5-cyclooctadiene) were carried out. Reactions in THF with a 1:1 ratio produced a complex with the formula $[Pd(C_6F_5)_2(Me\text{-}BPzTOMe)]$ (**8**) containing the unaltered triazine ligand (see Scheme 3). However, when 2 equiv of palladium was added, compound **8**, which is instantaneously formed in the solution, slowly evolves to give unidentified decomposition products of the ligand according to a study monitored by ^{1}H NMR in acetone-d_6 solution. The reaction of $[Pd(C_6F_5)_2(cod)]$ with Me-TPzT, both in 1:1 and 2:1 ratios, leads to unidentified complex mixtures.

(18) *International Tables for X-ray Crystallography*; Kynoch Press: Birmingham, England, 1974; Vol. IV.

(19) The water necessary for the hydrolysis must arise from the silver salts and perhaps also from traces in the solvent. We have tried to completely remove all water from $AgPF_6$, but it has proved impossible, even after drying over P_2O_5 with a vacuum higher than 10^{-2} mmHg during 5 days. Similar results have been reported: Horn, E.; Snow, M. R. *Aust. J. Chem.* **1980**, *33*, 2369.

(20) (a) Illuminati, G. *Adv. Heterocycl. Chem.* **1964**, *3*, 285. (b) Illuminati, G.; Stegel, F. *Adv. Heterocycl. Chem.* **1983**, *34*, 305. (c) Cramton, M. R. *Adv. Phys. Org. Chem.* **1969**, *7*, 211. (d) Terrier, F. *Chem. Rev.* **1982**, *82*, 78. (e) Bernasconi, C. F.; Muller, M. C. *J. Am. Chem. Soc.* **1978**, *100*, 5530. (f) Manderville, R. A.; Buncel, E. *J. Chem. Soc., Perkin Trans. 2* **1993**, 1887. (g) Manderville, R. A.; Buncel, E. *J. Am. Chem. Soc.* **1993**, *115*, 8985. (h) Terrier, F. *Nucleophilic Aromatic Displacement: Influence of the Nitro group*; VCH: Weinheim, Germany, 1991. (i) Buncel, E.; Crampton, M. R.; Strauss, M. J.; Terrier, F. *Electron Deficient Aromatic and Heterocyclic-Base Interactions*; Elsevier: Amsterdam, 1984. (j) Pietra, F. *Q. Rev. Chem. Soc.* **1969**, *23*, 504. (k) Miller, J. *Aromatic Nucleophilic Substitution*; Elsevier: Amsterdam, 1968.

(21) (a) Renfrew, A. H. M.; Taylor, J. A.; Whitmore, J. M. J.; Williams, A. *J. Chem. Soc., Perkin Trans. 2* **1994**, 2383. (b) Renfrew, A. H. M.; Rettura, D.; Taylor, J. A.; Whitmore, J. M. J.; Williams, A. *J. Am. Chem. Soc.* **1995**, *117*, 5484. (c) Cullum, N. R.; Renfrew, A. H. M.; Rettura, D.; Taylor, J. A.; Whitmore, J. M. J.; Williams, A. *J. Am. Chem. Soc.* **1995**, *117*, 9200. (d) Thomas, N. C.; Foley, B. L.; Rheingold, A. L. *Inorg. Chem.* **1988**, *27*, 3426.

Characterization of 1−8. Complexes **1**−**8** were characterized by NMR and IR spectroscopy, by elemental analysis (except for **7**), and, in some cases, by FAB MS. ^{1}H and ^{13}C-{^{1}H} NMR data of the complexes at room temperature, along with those of the starting ligands, are compiled in Tables 1 and 2. For complex **1**, pyrazolic and allylic signals have been assigned after NOE experiments and a one-bond carbon−proton correlation has allowed the assignment of the ^{13}C resonances. The resonances of the other complexes have been assigned by comparison with **1**. Complexes **1**−**4** only differ in the nature of the anion, and their ^{1}H and ^{13}C{^{1}H} NMR spectra are identical. All data for **1**−**5** and **7** indicate a highly symmetric structure with only one type of pyrazole. Besides, for **1**−**4** the triazine C_4 and C_6 carbons appear equivalent (these carbons are not observed in **5**). The ^{1}H NMR spectrum of **6** shows four broad signals for the aromatic protons, indicating that two different pyrazolyl groups are present. The corresponding carbon resonances are also broad. The ^{1}H NMR resonances of one pyrazole are shifted to higher frequencies as a consequence of its coordination to the palladium center.

In the complexes described thus far, although asymmetric allylic groups are expected, the H_{anti}, H_{syn}, and terminal allylic carbons give rise to either two broad signals or a unique signal in each case. These observations have been shown to be indicative of a fluxional behavior in similar allylpalladium complexes with N-donor ligands.[12b] The observation of broad proton and carbon signals for the two different pyrazolyl groups in **6** also indicates a possible dynamic process that interconverts both groups. Consequently, a variable-temperature ^{1}H NMR study was carried out for **1** and **6** (see below).

Both the ^{1}H and ^{13}C{^{1}H} NMR of **8** indicate the existence, at room temperature, of two distinct pyrazolyl groups. One of these groups must be free and the other coordinated to the palladium center. In the ^{19}F NMR spectrum two different and freely rotating C_6F_5 groups are seen (see the Experimental Section).

A significant fact observed in the IR spectra of **1**−**5** is the presence of a ν(C═O) band at about 1790 cm^{-1}. This is a consequence of the partial hydrolysis process of the TPzT ligands. This is a very high wavelength considering the amidic character of the functional group; for instance, it represents a shift of 95 cm^{-1} from cyanuric acid.[22] This marked shift confirms the double bond character of the C═O group due to the coordination of the adjacent nitrogen atoms to the palladium centers. The existence of this bond has also been confirmed by the X-ray structure determination of this compound (see below).

The FAB mass spectra of **1** and **5** both show a similar pattern. The more characteristic peaks are those corresponding to $[M]^+$, $[M - C_4H_7]^+$ and $[M - C_4H_7Pd]^+$. Unfortunately, the mass spectrum of a highly enriched sample of **7** is identical to that of **1**. This indicates the ease of hydrolysis of the Me-BPzTOMe ligand when coordinated to two allyl−Pd fragments and also the high stability of the corresponding cation formed. In contrast, the FAB mass spectrum of **6** does not show peaks corresponding to fragments containing hydrolyzed ligand. The most relevant peaks are those corresponding to the cation $[M]^+$ and $[M - C_4H_7]^+$. The FAB mass spectrum of **8** provides new data about the origin of the hydrolysis in this type of ligand. In this spectrum some of the peaks that appear correspond to a hydrolyzed ligand ($[M - Me]^+$, $[M - Me - pz]^+$, and $[M - Me - pz - C_6F_5]^+$) whereas two other fragment peaks, corresponding to the loss of C_6F_5 groups, are due to the unchanged ligand ($[M - C_6F_5]^+$ and $[M - 2(C_6F_5)]^+$). This is consistent with the expected decrease in the acceptor character of the metallic center when C_6F_5 fragments are lost and, as a consequence, the triazine ring is then less sensitive to nucleophilic attack by water.

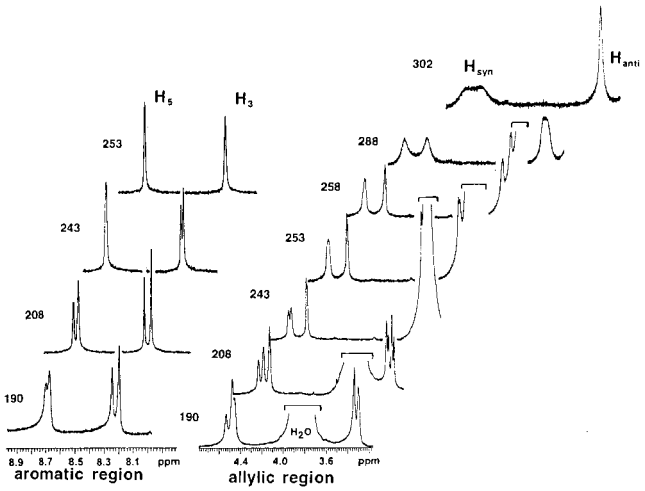

Figure 1. Variable-temperature ^{1}H NMR study of complex **1** in the aromatic and allylic region. Temperatures are in K. In the aromatic region the *meso* ↔ *dl* isomer exchange, which is represented in Scheme 4, is shown. In the allylic region a simultaneous *syn*−*syn*, *anti*−*anti* exchange of these two isomers is visualized.

Fluxional Behavior of Complexes 1 and 6. Complex 1. The ^{1}H NMR spectrum of **1** at room temperature in acetone-d_6 exhibits the signals for the H_{syn} and H_{anti} protons of the allyl group as two broad signals and a broad singlet, respectively. When the temperature is increased, the H_{syn} signals evolve to give a singlet beyond its coalescence. The H_{syn} signals are split and finally four resonances, which are not completely separated, are seen (see Figure 1) at low temperature in such a way that several coalescences are observed. The same effect is observed for H_{anti}. Similarly, the signals due to the pyrazolic H_3 and H_5 protons, the methyl allyl groups, and the Me-BPTO group are split into two signals at low temperatures. The calculated free activation energies[15] at the coalescences ($\Delta G_c^{\ddagger}$) and the corresponding temperatures are shown in Table 3. The different activation energies $\Delta G_c^{\ddagger}$ determined in this way are related in a linear fashion with the coalescence temperatures ($r^2 = 0.92$). This fact agrees with the existence of a unique fluxional process. To account for these observations we propose the existence of three stereoisomers, a *meso* form and a *d*,*l* pair of enantiomers (see Scheme 4). Each isomer has two equivalent asymmetric allyl groups and two identical pyrazole rings. The molecular structure of the *meso* form has been determined by an X-ray diffraction study (see below). Other isomers, of lower symmetry, containing one allylpalladium fragment bonded to a pyrazole group and to the N_5 of the triazine may be excluded on the basis of the steric hindrance of the allyl group with the pyrazole ring coordinated to the other palladium center. Besides, considering that the *meso* form is present, the simultaneous existence of the asymmetric isomer would lead to a higher number of signals than is actually observed in the ^{1}H NMR spectrum.

When the variable-temperature ^{1}H NMR study of **1** was carried out in dichloromethane-d_2, similar changes were observed in the resonances and the calculated $\Delta G_c^{\ddagger}$ values are slightly higher, indicating a possible coordinative participation of the acetone molecules in the fluxional process. Moreover, the addition of chloride ions to the dichloromethane solution

(22) Pouchet, C. J. *The Aldrich Library of Infrared Spectra*, 3rd ed.; Aldrich Chemical Co., Inc.: Milwaukee, WI, 1981; p 1380 G.

Scheme 4

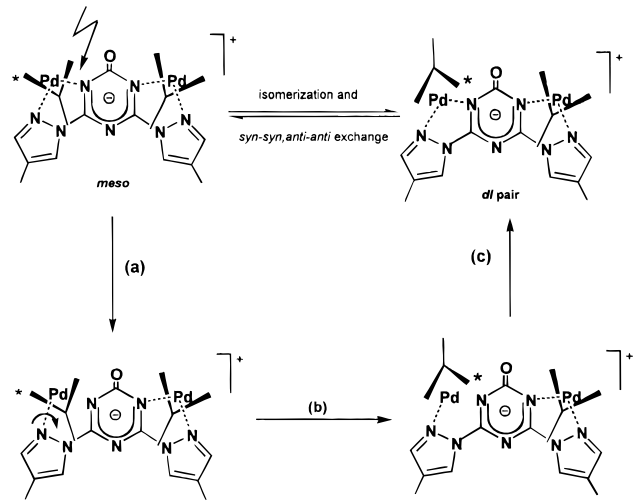

noticeably accelerates the interchange. The formation of the known $[Pd(\eta^3\text{-}C_4H_7)Cl]_2$ dimer is also observed after this addition as a consequence of a dissociative process.

Several mechanisms have been proposed for the isomerization or *syn*−*syn* and *anti*−*anti* interchange in (η^3-allyl)palladium complexes.[23] A simple rotation of the allyl ligand in its plane about an axis containing the metal center is usually excluded in square-planar geometries.[23b] Some authors[24] support an associative mechanism for this apparent allyl rotation, while in some complexes with N-donor ligands a dissociative pathway has been proposed[25] by others and also by ourselves.[12] The rate enhancement effect produced by addition of chloride anions (and also of the acetone solvent) has been used as an argument supporting both dissociative (stabilization of tricoordinate intermediates)[25b] and associative (formation of the pentacoordinated intermediate) pathways.[24b] We think that in complexes such as **1** the Pd−N bond rupture is a very probable occurrence for the following two reasons. First, in two allyl complexes with pyrazole-containing ligands,[12b] which are similar to those reported in this work, we have proved without ambiguity, through the observation of NOEs between H_{anti} and protons situated far away from the coordination center, that the Pd−N bond rupture and internal rotation of the ligand take place. In addition, in complex **6**, whose dynamic behavior is described below, it is clear that Pd−N bond cleavage occurs. Second, the free activation parameters for **1** resemble the values described for these types of complexes where dissociative pathways are proposed.[25,12] The whole process may be explained as depicted in Scheme 4 and proceeds according to the following steps: (a) dissociation of a Pd−N bond, (b) isomerization and Pd−N bond rotation of the tricoordinated intermediate,[26] and (c) reformation of the Pd−N bond. Cleavage of the Pd−N(triazine) bond is reflected in Scheme 4, but we have no data to exclude the possibility of the rupture of the Pd−N(pyrazole) bond. The proposed mechanism simultaneously explains the *syn*−*syn* and *anti*−*anti* interchange and also the observed isomerization process.

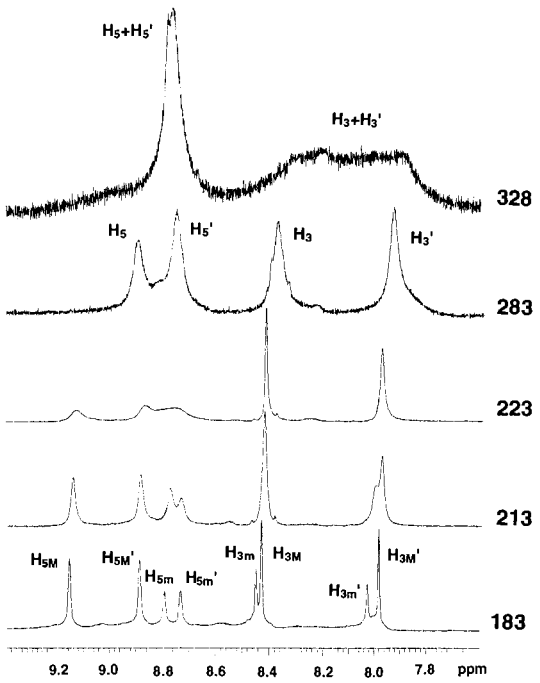

Figure 2. Variable-temperature ^{1}H NMR study of complex **6** (see Table 3) in the aromatic region. Temperatures are in K. At 283 K equilibrium i (see Scheme 5) exchanges the corresponding **6a**,**b** signals. At 328 K equilibrium ii exchanges coordinated and noncoordinated pyrazole resonances. M and m refers to the major and minor isomers of **6**.

Complex 6. The broad resonances of the aromatic protons at room temperature become even broader when the temperature of the acetone solution is increased, and this continues until the corresponding coalescences between the signals of the coordinated and noncoordinated pyrazoles are reached (see Table 3 and Figure 2). At low temperatures (205 K) (Figure 2), two different species in an approximately 60:40 ratio are seen with resonances for two distinct pyrazoles in each case (see Table 1). The identification of the protons and methyl groups that belong to the same pyrazolyl group has been performed by a COSY experiment. Two signals are also observed for the methoxy group, but the expected resonances for the allylic protons are not resolved. We propose that these two species are **6a**,**b** and that these are in fast interconversion at room temperature (see Scheme 5). Although we have made great efforts, by means of NOE studies at low temperature, we have not been able to assign the observed resonances to a particular species. One reason could be the low solubility of **6** at low temperature. However, it is also reasonable that the noncoordinated pyrazole in **6b** will be twisted out of the triazine plane in order to avoid steric interaction with the allylpalladium fragment, thus making it difficult to observe NOE between these groups.[27]

(23) (a) Maitlis, P. M.; Espinet, P.; Russell, M. J. H. In *Comprehensive Organometallic Chemistry*; Wilkinson, G., Stone, F. G. A., Abel, E. W., Eds.; Pergamon Press: Oxford, U.K., 1982; Vol. 6, p 385. (b) K. Vrieze In *Dynamic Nuclear Magnetic Resonance Spectroscopy*; Jackman, L. M., Cotton, F. A., Eds.; Academic Press: New York, 1975.

(24) (a) Crociani, B.; Di Bianca, F.; Giovenco, A.; Boschi, T. *Inorg. Chim. Acta* **1987**, *127*, 169. (b) Hansson, S.; Norrby, P. O.; Sjögren, M. P. T.; Åkermark, B.; Cucciolito, M. E.; Giordano, F.; Vitagliano, A. *Organometallics* **1993**, *12*, 4940. (c) Crociani, B.; Antonaroli, S.; Paci, M.; Di Bianca, F.; Canovese L. *Organometallics* **1997**, *16*, 384.

(25) (a) Albinati, A.; Kunz, R. W.; Amman, C. J.; Pregosin, P. S. *Organometallics* **1991**, *10*, 1800. (b) Gogoll, A.; Örnebro, J.; Grennberg, H.; Bäckvall, J. E. *J. Am. Chem. Soc.* **1994**, *116*, 3631. (c) Gogoll, A.; Grennberg, H.; Axén, A. *Organometallics* **1997**, *16*, 1167.

(26) (a) Thorn, D. L.; Hoffmann, R. *J. Am. Chem. Soc.* **1978**, *100*, 2079. (b) Alibrandi, G. Scolaro, L. M.; Romeo, R. *Inorg. Chem.* **1991**, *30*, 4007. (c) Tatsumi, K.; Hoffmann, R.; Yamamoto, A.; Still, J. K. *Bull. Chem. Soc. Jpn.* **1981**, *54*, 1857.

(27) For example, in the X-ray structure of the complex $[PtIMe_3(dmpbipy)]$ [dmpbipy = 6-(3,5-dimethylpyrazol-1-yl)-2,2′-bipyridine], the pyrazolyl ring that it is not involved in the coordination is twisted out of the bipy plane: Gelling, A.; Orrell, K. G.; Osborne, A. G.; Sik, V.; Hursthouse, M. B.; Coles, S. J. *Polyhedron* **1996**, *15*, 3203.

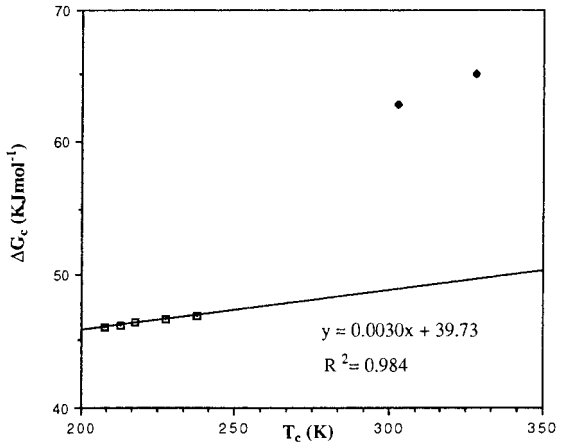

Figure 3. Linear plot of $\Delta G_c^{\ddagger}$ (kJ mol^{-1}) versus T_c (K) for complex **6** (see Table 3): (□) exchange of **6a**,**b** resonances; (◆) exchange of free and coordinated pyrazole resonances.

Scheme 5

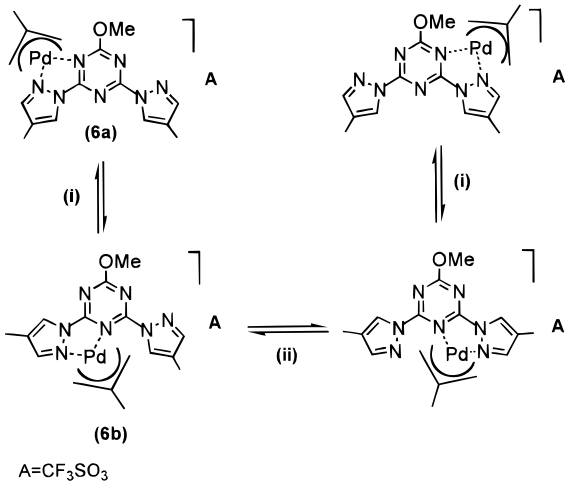

Between 208 and 238 K several coalescences of the pyrazolyl signals are observed (see Table 3) that correspond to interchange of resonances of the major isomer with those of the minor isomer, without changing the character of the free or coordinated pyrazolyl groups. The plot of the $\Delta G_c^{\ddagger}$ values against T_c fits a straight line very well, suggesting the same activation barrier for these exchanges (Figure 3). However, the $\Delta G_c^{\ddagger}$ values corresponding to the interchange between free and coordinated pyrazolyl protons (T_c above room temperature) are considerably higher than expected for this linear plot (see Figure 3). This fact is very conclusive and clearly indicates a different pathway for the two types of observed exchanges. If we consider Scheme 5, it is possible to observe that the interchange between **6a** and **6b** (path i) can occur through a Pd−N(triazine) bond rupture accompanied by a 180° rotation of the metal−pyrazolyl group about the C−N bond, while the change of the allylpalladium fragment from one pyrazolyl group to the other (path ii), which can take place by a 1,4 metallotropic shift,[28] needs the cleavage of the Pd−N(pyrazolyl) bond. A full dissociation of the metal center followed by a recombination in a different position can be excluded because it would lead to a unique activation barrier for both types of interchange. From the evidence described above it is reasonable to propose that the Pd−N bond rupture is the process that has most influence on the activation barrier of each process and that this bond is stronger when the pyrazolyl nitrogen atom is involved. This hypothesis fits in well with the corresponding basicities[29] for the parent heterocycles. A similar metallotropic process has been reported by Orrell et al.[30] for 2,4,6-tris(2-pyridyl)-1,3,5-triazine (tpt) and 2,4,6-tris(2-pyridyl)-pyrimidine coordinated to palladium or platinum fragments containing fluorinated aryl groups. In these cases, the activation barriers are considerably higher, both for paths i and ii, than those found by us and they have only been measured on the basis of EXSY experiments. In our case, the difference in the energy barriers between the two processes is considerably higher.

Another interesting conclusion can be drawn after the comparison of the $\Delta G_c^{\ddagger}$ data for complexes **1** and **6** (see Table 3). The low barrier corresponding to the Pd−N(triazine) bond rupture of complex **6** does not correspond with any $\Delta G_c^{\ddagger}$ value of complex **1**. In fact, all the values for this last derivative are above the barriers related to the Pd−N(pyrazolyl) bond rupture in complex **6**. This denotes that in **1** the Pd−N(triazine) bond is notably stronger that in **6**. The reason for this must be the anionic character of the Me-BPzTO ligand and the delocalization of the electronic charge in the triazine ring. Consequently, the ease of hydrolysis of the Me-TPzT, Br-TPzT, and Me-BPzTOMe ligands, in the presence of the allylpalladium fragment, may have its origin in the bond reinforcement of the triazine with the palladium center.

Complex 8. To assess the influence of the electrophilic character of the metallic fragment on the fluxional behavior, a variable temperature study in toluene-d_8 solution was carried out for complex **8**. Only one compound was observed over the whole temperature range studied (183−373 K), which does not indicate interchange of free and coordinated pyrazole rings. This reflects the rigid character of complex **8**. The main difference between **8** and **6** is the electrophilic character of the palladium center and, as a consequence, the strength of the Pd−N bond. This again suggests a significant influence of the Pd−N bond rupture in the mechanism for this type of dynamics. Although a structure similar to **6a** has been proposed for the static structure of **8** (see Scheme 3), the possibility of having the metallic center in a disposition similar to that in **6b** cannot be totally rejected. The former structure seems to be more reasonable considering steric reasons and the higher basicity of the triazine N_1 atom in comparison to N_5.

X-ray Structure of 4. To support our studies of the complexes in solution, we determined the molecular structure of **4** by X-ray diffraction. The crystal structure consists of a dinuclear Pd cation and *p*-toluenesulfonate counterion. An ORTEP plot of the cation is shown in Figure 4, and a selected list of bond lengths and angles is given in Table 5.

The cation lies on a crystallographic mirror plane containing the atoms O(5), C(13), and N(8), so that only half of the molecule is crystallographically independent. The geometry

(28) For some examples of 1,4-metallotropic shifts in square-planar complexes see: (a) Abel, E. W.; Orrell, K. G.; Osborne, A. G.; Pain, H. M.; Sik, V.; Hursthouse, M. B.; Malik, K. M. A. *J. Chem. Soc., Dalton Trans.* **1994**, 3441. (b) Abel, E. W.; Gelling, A.; Orrell, K. G.; Osborne, A. G.; Sik, V. *J. Chem. Soc., Chem. Commun.* **1996**, 2329. (c) Rotondo, E.; Giordano, G.; Minniti, D. *J. Chem. Soc., Dalton Trans.* **1996**, 253 (letter).

(29) As a reference, pyrazole is 56.0 kJ/mol more basic than triazine: (a) Meot-Ner, M. *J. Am. Chem. Soc.* **1979**, *101*, 2396. (b) Abboud, J. L. M.; Cabildo, P.; Cañada, T.; Catalán, J.; Claramunt, R. M.; de Paz, J. L. G.; Elguero, J.; Homan, H.; Toiron, C.; Yranzo, G. I. *J. Org. Chem.* **1992**, *57*, 3938.

(30) (a) Gelling, A.; Olsen, M. D.; Orrell. K. G.; Osborne, A. G.; Sik, V. *J. Chem. Soc., Chem. Commun.* **1997**, 587. (b) Gelling, A.; Oken, M. D.; Orrell, K. G.; Osborne, A. G.; Sik, V. *Inorg. Chim. Acta* **1997**, *264*, 257.

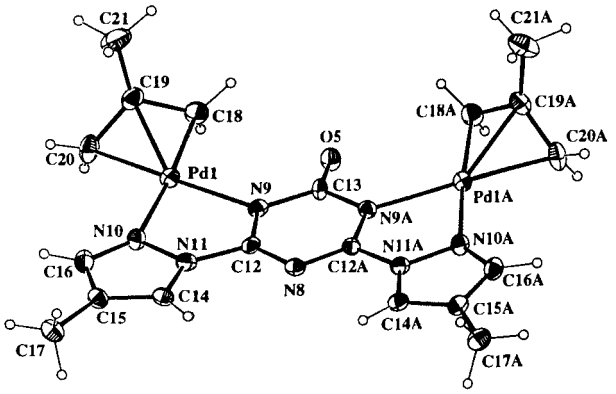

Figure 4. ORTEP view with atomic numbering of the cation $[\{(\eta^3\text{-}2\text{-Me-}C_3H_4)Pd\}_2(Me\text{-}BPzTO)]^+$ (cation of **4**).

Table 5. Selected Bond Distances (Å) and Bond Angles (deg) of Compound **4**

Pd(1)−N(10)	2.092(5)	N(10)−N(11)	1.376(7)
Pd(1)−N(9)	2.106(5)	N(11)−C(14)	1.345(8)
Pd(1)−C(19)	2.129(7)	N(11)−C(12)	1.396(8)
Pd(1)−C(18)	2.119(7)	C(13)−N(9A)	1.402(7)
Pd(1)−C(20)	2.113(7)	C(14)−C(15)	1.360(9)
O(5)−C(13)	1.212(11)	C(15)−C(16)	1.411(9)
N(8)−C(12)	1.314(7)	C(15)−C(17)	1.506(10)
N(8)−C(12A)	1.314(7)	C(18)−C(19)	1.423(10)
N(9)−C(12)	1.323(8)	C(19)−C(20)	1.402(12)
N(9)−C(13)	1.402(7)	C(19)−C(21)	1.526(13)
N(10)−C(16)	1.311(8)		
N(10)−Pd(1)-N(9)	77.8(2)	O(5)−C(13)-N(9)	121.7(4)
N(9)−Pd(1)-C(18)	106.8(3)	N(9)−C(13)-N(9A)	116.6(8)
N(10)−Pd(1)-C(20)	107.1(3)	C(20)−C(19)-C(18)	114.9(8)
C(18)−Pd(1)-C(20)	68.5(3)	C(20)−C(19)-C(21)	120.8(8)
C(12)−N(8)-C(12A)	112.0(7)	C(18)−C(19)-C(21)	122.8(8)
C(12)−N(9)-C(13)	117.2(6)	C(21)−C(19)-Pd(1)	117.4(6)
N(9)−C(12)-N(8)	128.5(6)		

around the Pd(1) atom is approximately square planar, and the five-membered chelate ring, including the Pd atom, shows only very small deviations from planarity. The Pd(1)−N(9) and Pd(1)−N(10) bonds form the basis for the five-membered chelate ring, and the distances are essentially equivalent [Pd(1)−N(9), 2.106(5) Å; Pd(1)−N(10), 2.092(8) Å]. The Pd−η^3-allyl distances are the following: Pd(1)−C(18) = 2.119(8) Å; Pd(1)−C(19) = 2.128(8) Å; Pd(1)−C(20) = 2.112(7) Å. These latter values are in the range expected for a Pd(II)−allyl with nitrogen ligands in trans positions. If we define a plane containing the Pd and the two nitrogen atoms N(9) and N(10) (coordination plane), then the terminal carbons are 0.065 Å [C(18)] below the plane and 0.175 Å [C(20)] above the plane and the central allyl carbon [C(19)] is 0.647 Å below it. The dihedral angle between the allylic plane and the palladium coordination plane is 111.3°, with the C(central) to $-CH_3$ vector pointing away from the metal. The bond length of C(13)−O(5) [1.21(1) Å] indicates the double-bond character of the C−O linkage. The triazine ring C−N distances at C(13) are typical single-bond values (1.40 Å), and the remaining four C−N distances are narrowly spread in the double-bond range [the C(12)−N(9) and C(12)−N(8) distances are 1.323(8) and 1.314(7) Å, respectively]. In addition, the central C_3N_3 ring is nearly planar, supporting pentadienide-delocalized bonding for the five atoms N(9), C(12), N(8), C(12A), and N(9A). The pyrazolyl rings coordinated to the palladium atoms are nearly coplanar with the triazine ring (dihedral angle of 1.81°).

Conclusions

We have shown that allylpalladium fragments may induce the partial hydrolysis of some pyrazole derivatives of triazine. The presence of two coordinated metallic moieties facilitates the process, and the better leaving character of pyrazolate in comparison to methoxy groups is observed. From the free activation energies at the coalescence temperatures, calculated from ^{1}H NMR studies, it is concluded that the main driving force for the hydrolysis is the improvement in the coordination ability of ligands. For complex **6** we have found an example in which the metal moiety moves completely around the outside of the triazine ring, adopting all the coordination possibilities involving nitrogen atoms. The calculation of the different $\Delta G_c^{\ddagger}$ values for the observed coalescences in a variable temperature ^{1}H NMR study shows that two different barriers are involved in the fluxional phenomenon. The corresponding energies for these two barriers correlate with the different strengths of the Pd−N bond to be broken (Pd−triazine or Pd−pyrazole) in the fluxional process and thus strongly support the importance of the Pd−N bond rupture in fluxional processes of allylpalladium complexes with N-donor ligands.

Acknowledgment. We gratefully acknowledge financial support from the Dirección General de Investigación Científica y Técnica (DGICYT) (Grants No. PB95-0901 and PB94-0742) of Spain. We also thank Dr. Mariano Laguna from the University of Zaragoza, Zaragoza, Spain, who recorded the mass spectra.

Supporting Information Available: X-ray crystallographic files, in CIF format, for complex **4** are available on the Internet only. Access information is given on any current masthead page.

IC980307N